An Analytical Model for IEEE 802.11 Point-to-Point Link

Yong Yan, Xiaowen Chu
Department of Computer Science, Hong Kong Baptist University
Email: {yyan, chxw}@comp.hkbu.edu.hk

Abstract **- Wireless mesh networks have attracted extensive research interests in recent years. With the maturity and pervasive deployment of IEEE 802.11a/b/g technology, 802.11 DCF protocol is considered as a promising candidate for constructing the backbone of wireless mesh networks. In a multi-channel multi-interface wireless mesh network, point-to-point 802.11 wireless link can provide the highest throughput; hence it is critical to understand the 802.11 throughput performance in a point-to-point configuration. This paper presents a simple yet precise Markov model for the analysis of point-to-point 802.11 link performance in terms of saturation throughput. Different from previously proposed analytical models, our model does not assume a constant and independent collision probability. Our analytical model is validated by computer simulations for both 802.11b and 802.11g configurations.**

I. Introduction

Wireless mesh networks (WMNs) are gaining significant progress in both academia research and commercial deployment in recent years [6, 7]. It has been shown that the aggregated system throughput can be significantly improved by exploiting multi-channel and multi-interface technique [8, 9, 10, 11]. A typical wireless mesh network is shown in Fig. 1, whose backbone consists of a set of wireless mesh routers. Wireless stations (i.e., end users) can access the Internet by associating with a nearby wireless mesh router. With a suitable channel assignment scheme and the help of directional antenna, it is possible that two nearby wireless mesh routers are connected by dedicated point-to-point wireless channel. This can greatly increase the capacity of wireless mesh backbone because each channel is shared by only two wireless mesh routers.

IEEE 802.11 is almost pervasively deployed by wireless LANs nowadays. The supported data rate of 802.11 has also been increased from 11Mbps (802.11b) and 54Mbps (802.11a/g) to 300Mbps or even 600Mbps (802.11n) [1, 2, 3]. It is therefore very promising to use IEEE 802.11 protocol in wireless mesh networks. Due to the limited number of wireless channels, it is very critical to improve the utilization of the scarce wireless spectrum. Our paper aims to analyze the saturation throughput of IEEE 802.11 point-to-point link, and also to find a suitable system parameter which can lead to the maximum saturation throughput.

The performance of IEEE 802.11 has been actively studied in the last years. Most of them focus on the scalability of 802.11 DCF, i.e., how to handle a large number of wireless stations. Cali et al. [4] derives an analytical model for 802.11 DCF using a *p*-persistent backoff scheme to approximate the original binary exponential backoff scheme. Bianchi [5] proposes a Markov chain model to derive the saturation throughput by assuming a constant and independent collision probability of a packet transmitted by each station. This assumption is accurate only when the number of stations in the wireless LAN is fairly large, however.

Our paper aims to develop a precise analytical model to calculate the saturation throughput of an 802.11 point-to-point link. The main difference between our model and existing models is that, our model does not make the assumption that the collision probability is constant and independent. Instead, our model makes a simple assumption that $CW_{max} = 2CW_{min}$. This assumption is reasonable for a point-to-point wireless link, as we will show by computer simulations that the saturation throughput is almost a constant value for all integers of $m \geq 1$ where $CW_{max} = 2^m CW_{min}$. Our model achieves better accuracy as compared with the well known Bianchi's model [5].

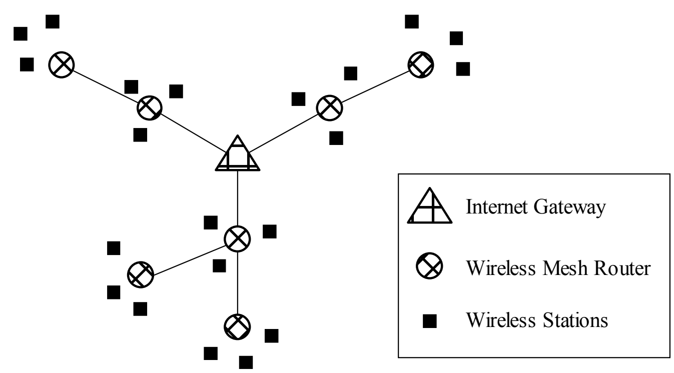

Figure 1: A multi-channel multi-interface wireless mesh network

The rest of the paper is organized as follows. Section II briefly reviews the 802.11 Distributed Coordination Function (DCF) protocol. Section III presents a Markov model used to calculate the saturation throughput for a point-to-point 802.11 DCF link. In Section IV, we validate our model by comparing with simulation results, for both 802.11b and 802.11g configurations. Finally, Section V concludes the paper.

II. Distributed Coordination Function (DCF)

The IEEE 802.11 standard is working on both the physical (PHY) and medium access control (MAC) layers of the network. Other than considering about the physical details, we will concentrate on the MAC layer protocol itself.

978-1-4244-2075-9/08/$25.00 ©2008 IEEE

The basic access method in the 802.11 MAC protocol is DCF (Distributed Coordination Function) known as carrier sense multiple access with collision avoidance (CSMA/CA) [1]. DCF employs a distributed CSMA/CA algorithm and an optional virtual carrier sense using RTS and CTS control frames. When using the DCF, before initiating a transmission, a station senses the channel to determine whether another station is transmitting. If the medium is found to be idle for an interval that exceeds the Distributed InterFrame Space (DIFS), the station proceeds with its transmission. However if the medium is busy, the transmission is deferred until the ongoing transmission terminates. A random interval, henceforth referred to as the backoff interval, is then selected; and used to initialize the backoff timer. The backoff timer is decreased as long as the channel is sensed idle, stopped when a transmission is detected on the channel, and reactivated when the channel is sensed idle again for more than a DIFS. The station transmits when the backoff timer reaches zero. CSMA/CA is a strategy that intends to avoid collisions, but it can not eliminate collisions. When more than one node are counting down their backoff timers, there's a probability that some of them have their timers reach zero at the same time slot, and start transmitting at the beginning of next time slot simultaneously, which causes a collision. The collision probability increases with the number of active senders in the network.

DCF requires each sender to wait for a random backoff period after the channel is idle for DIFS, it adopts a slotted binary exponential backoff scheme. The backoff time is calculated as *BackoffTime = Random() × aSlotTime* where *Random()* indicates a uniformly distributed random integer between $[0, CW-1]$ and CW represents the value of contention window, which starts from $CW_{\min}$, doubled each time a retransmission occurs, until reaching the maximum value $CW_{\max}$.

III. Analytical Model of DCF

We consider a simple ad hoc wireless network that consists of two nodes, that is, a point-to-point network. The pre-assumptions of our model are: (1) only two nodes are in the network; (2) each node always has packets to send to the other one; (3) the probability density function of both nodes' backoff timers are uniformly distributed in the same range, which means that both nodes are competing for the channel equally. In our model, we set the CW_{max} as twice of CW_{min}, which indicates a 2-level exponential backoff scheme. Although the IEEE 802.11g standard defines a multi-level exponential backoff scheme where $CW_{max} = 2^m CW_{min}$, we will show that there is negligible difference between 2-level and multi-level schemes for a point-to-point wireless link.

A. *The Markov System Model*

We use a Markov chain to model the network with two nodes. Each node has a backoff timer. Our model focuses on the difference between two backoff timers. Let each state in the Markov chain be the current absolute difference, in unit of time slots, between the two backoff timers. For instance, state *i* represents that currently the backoff timer of one sender is *i* time slots longer than another sender's backoff timer. Apparently, collision will happen at state 0, because the two senders have the same backoff timers and they will transmit their packets simultaneously. On the other hand, every non-zero state implies a successful transmission. Fig. 2 shows the Markov chain model, in which all states are divided into two levels: the states from 0 to $CW_{\min}-1$ belong to the Low-Level, while the states from $CW_{\min}$ to $CW_{\max}-1$ belong to the High-Level.

Let $P\{j \mid i\}$ denote the transition probability from state *i* to state *j*. Then the transition probabilities are:

$$P\{j \mid i\} = 1/CW_{max},\ i = 0,\ j = 0 \tag{1}$$

$$P\{j \mid i\} = 2(CW_{\max} - j)/CW_{\max}^{2},\ i = 0,\ j \in [1, W_{\max} - 1] \tag{2}$$

$$P\{j \mid i\} = 1/CW_{\min},\quad i \in [1, CW_{\min} - 1],\ j = 0 \tag{3}$$

$$P\{j \mid i\} = 2/CW_{\min},\ i \in [j, CW_{\min} - 1 - j],\ j \in [1, (CW_{\min}/2) - 1] \tag{4}$$

$$P\{j \mid i\} = 1/CW_{\min}, i \in [1, (CW_{\min}/2) - 1],\ j \in [i+1, CW_{\min} - 1 - i] \tag{5}$$

$$P\{j \mid i\} = 1/CW_{\min}, i \in [CW_{\min}/2, CW_{\min} - 1],\ j \in [CW_{\min} - i, i] \tag{6}$$

$$P\{j \mid i\} = 1/CW_{\min}, i \in [CW_{\min}, CW_{\max} - 1],\ j \in [i - CW_{\min} + 1, i] \tag{7}$$

At the Low-Level, since state 0 represents collisions, Eqs. (1) and (2) account for the process following a collision. In particular, $P\{0 \mid 0\}$ is the probability that system encounters two consecutive collisions. Eq. (3) represents the process that a successful transmission is followed by a collision. Eq. (4) accounts for the process of backward transition, which means a new random backoff timer makes a new difference that is smaller than the previous difference. In contrast, Eqs. (5) and (6) accounts for the forward transition.

Once the state is at CW_{min} or higher, the system is at the High-Level. A non-zero state always implies a successful transmission ahead, which will be followed by a selection of random number between 0 and $CW_{min}-1$. Therefore, all states in the High-Level can only have backward transitions to their previous CW_{min} states, which is represented by Eq. (7).

To illustrate the Markov model, the transition probability matrix for CW_{min} = 16 and CW_{max} =32 is shown in Fig. 3. In this matrix, *I* represents the value of $1/CW_{min}$, *X* represents the value of $2/CW_{min}$, and *Z* represents the value of $1/CW_{min}^{2}$. There are CW_{max} equations and CW_{max} unknown parameters in this matrix. If we denote each entry in this matrix as $m[i, j]$, and the solution to this matrix is $q[i]$, these equations can be written by:

$$q[j] = \sum_{i=0}^{CW_{\max}-1} q[i]m[i, j],\quad j \in [0, CW_{\max} - 1]. \tag{8}$$

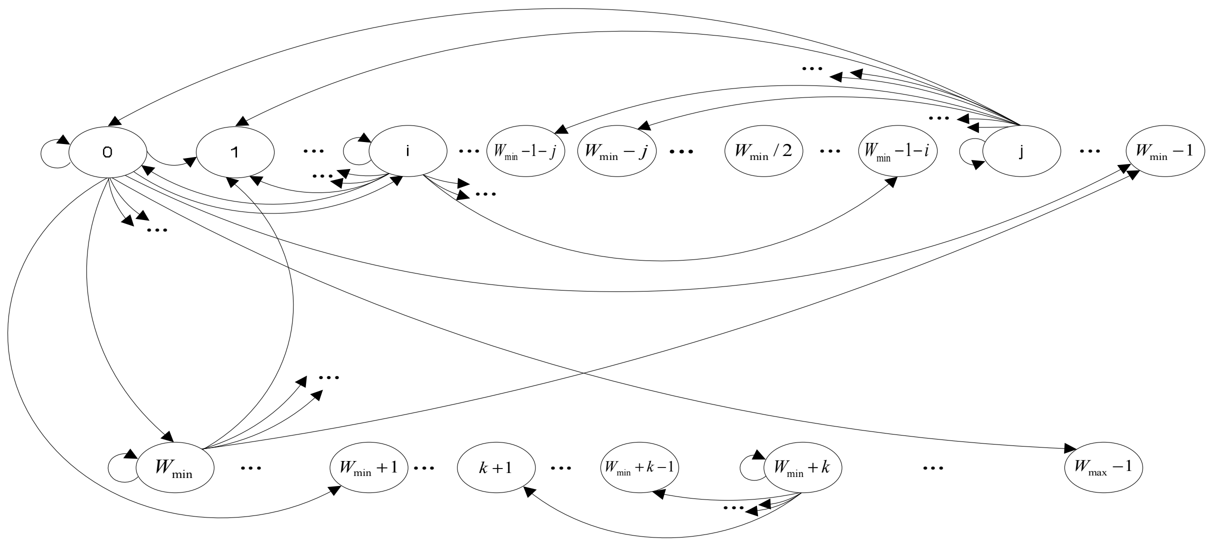

Figure 2: The Markov model (to save space, CW_{min} and CW_{max} are expressed as W_{min} and W_{max}, respectively)

According to the property of Markov chain, this matrix can be solved by numerical method. The solution *q[i]* denotes the probability that the difference between the two backoff timers is *i* time slots.

B. Distribution of System Idle time

We denote *X* and *Y* as the random variable of both random backoff timers. At the Low-Level, both nodes have their uniform distribution of random backoff timers: $f_x(X) = f_y(Y) = 1/CW_{\min}$, where *X* and *Y* range from 0 to $CW_{min}-1$. By solving the Markov matrix, we can get the probability distribution of the difference of backoff timers in two levels; and we denote the solution $q[i]$ as $f_i(|X'-Y'|)$.

```
       i:
j:        0,1,2,3,4,5,6,7,8,9,0,1,2,3,4,5,6,7,8,9,0,1,2,3,4,5,6,7,8,9,0,1
 0  {32*Z,I,I,I,I,I,I,I,I,I,I,I,I,I,I,I,0,0,0,0,0,0,0,0,0,0,0,0,0,0,0,0},
 1  {62*Z,X,X,X,X,X,X,X,X,X,X,X,X,X,X,I,I,0,0,0,0,0,0,0,0,0,0,0,0,0,0,0},
 2  {60*Z,I,X,X,X,X,X,X,X,X,X,X,X,X,I,I,I,0,0,0,0,0,0,0,0,0,0,0,0,0,0,0},
 3  {58*Z,I,I,X,X,X,X,X,X,X,X,X,X,I,I,I,I,I,0,0,0,0,0,0,0,0,0,0,0,0,0,0},
 4  {56*Z,I,I,I,X,X,X,X,X,X,X,X,I,I,I,I,I,I,I,0,0,0,0,0,0,0,0,0,0,0,0,0},
 5  {54*Z,I,I,I,I,X,X,X,X,X,X,I,I,I,I,I,I,I,I,I,0,0,0,0,0,0,0,0,0,0,0,0},
 6  {52*Z,I,I,I,I,I,X,X,X,X,I,I,I,I,I,I,I,I,I,I,I,0,0,0,0,0,0,0,0,0,0,0},
 7  {50*Z,I,I,I,I,I,I,X,X,I,I,I,I,I,I,I,I,I,I,I,I,I,0,0,0,0,0,0,0,0,0,0},
 8  {48*Z,I,I,I,I,I,I,I,I,I,I,I,I,I,I,I,I,I,I,I,I,I,I,0,0,0,0,0,0,0,0,0},
 9  {46*Z,I,I,I,I,I,I,0,0,I,I,I,I,I,I,I,I,I,I,I,I,I,I,I,0,0,0,0,0,0,0,0},
 10 {44*Z,I,I,I,I,I,0,0,0,0,I,I,I,I,I,I,I,I,I,I,I,I,I,I,I,0,0,0,0,0,0,0},
 11 {42*Z,I,I,I,I,0,0,0,0,0,0,I,I,I,I,I,I,I,I,I,I,I,I,I,I,I,0,0,0,0,0,0},
 12 {40*Z,I,I,I,0,0,0,0,0,0,0,0,I,I,I,I,I,I,I,I,I,I,I,I,I,I,I,0,0,0,0,0},
 13 {38*Z,I,I,0,0,0,0,0,0,0,0,0,0,I,I,I,I,I,I,I,I,I,I,I,I,I,I,I,0,0,0,0},
 14 {36*Z,I,0,0,0,0,0,0,0,0,0,0,0,0,I,I,I,I,I,I,I,I,I,I,I,I,I,I,I,I,0,0},
 15 {34*Z,0,0,0,0,0,0,0,0,0,0,0,0,0,0,I,I,I,I,I,I,I,I,I,I,I,I,I,I,I,I,0},
 16 {32*Z,0,0,0,0,0,0,0,0,0,0,0,0,0,0,0,I,I,I,I,I,I,I,I,I,I,I,I,I,I,I,I},
 17 {30*Z,0,0,0,0,0,0,0,0,0,0,0,0,0,0,0,0,I,I,I,I,I,I,I,I,I,I,I,I,I,I,I},
 18 {28*Z,0,0,0,0,0,0,0,0,0,0,0,0,0,0,0,0,0,I,I,I,I,I,I,I,I,I,I,I,I,I,I},
 19 {26*Z,0,0,0,0,0,0,0,0,0,0,0,0,0,0,0,0,0,0,I,I,I,I,I,I,I,I,I,I,I,I,I},
 20 {24*Z,0,0,0,0,0,0,0,0,0,0,0,0,0,0,0,0,0,0,0,I,I,I,I,I,I,I,I,I,I,I,I},
 21 {22*Z,0,0,0,0,0,0,0,0,0,0,0,0,0,0,0,0,0,0,0,0,I,I,I,I,I,I,I,I,I,I,I},
 22 {20*Z,0,0,0,0,0,0,0,0,0,0,0,0,0,0,0,0,0,0,0,0,0,I,I,I,I,I,I,I,I,I,I},
 23 {18*Z,0,0,0,0,0,0,0,0,0,0,0,0,0,0,0,0,0,0,0,0,0,0,I,I,I,I,I,I,I,I,I},
 24 {16*Z,0,0,0,0,0,0,0,0,0,0,0,0,0,0,0,0,0,0,0,0,0,0,0,I,I,I,I,I,I,I,I},
 25 {14*Z,0,0,0,0,0,0,0,0,0,0,0,0,0,0,0,0,0,0,0,0,0,0,0,0,I,I,I,I,I,I,I},
 26 {12*Z,0,0,0,0,0,0,0,0,0,0,0,0,0,0,0,0,0,0,0,0,0,0,0,0,0,I,I,I,I,I,I},
 27 {10*Z,0,0,0,0,0,0,0,0,0,0,0,0,0,0,0,0,0,0,0,0,0,0,0,0,0,0,I,I,I,I,I},
 28 { 8*Z,0,0,0,0,0,0,0,0,0,0,0,0,0,0,0,0,0,0,0,0,0,0,0,0,0,0,0,I,I,I,I},
 29 { 6*Z,0,0,0,0,0,0,0,0,0,0,0,0,0,0,0,0,0,0,0,0,0,0,0,0,0,0,0,0,I,I,I},
 30 { 4*Z,0,0,0,0,0,0,0,0,0,0,0,0,0,0,0,0,0,0,0,0,0,0,0,0,0,0,0,0,0,I,I},
 31 { 2*Z,0,0,0,0,0,0,0,0,0,0,0,0,0,0,0,0,0,0,0,0,0,0,0,0,0,0,0,0,0,0,I},
```

Figure 3: Transition Probability Matrix

With the above solution, we are now ready to calculate the system throughput. In terms of throughput analysis, what really matters is the system idle time cost by the random backoff period, and this idle time always equals the shorter backoff timer at each transmission round. In other words, we are about to use the solution $f_i(|X'-Y'|)$ to find the probability p_j, which is the probability that system is idle for *j* time slots in one transmission round, and it can be calculated as following:

$$p_j = q[0]/CW_{\min} + (1-q[0])/CW_{\min} = 1/CW_{\min}, \quad j = 0 \tag{9}$$

$$p_j = \sum_{i=j}^{CW_{\max}-1} q[i]/CW_{\min} + q[j](CW_{\min}-1-j)/CW_{\min} + q[0](1/CW_{\max}{}^2 + 2(CW_{\max}-1-j)/CW_{\max}{}^2), \quad j \in [1, CW_{\min}-1] \tag{10}$$

$$p_j = q[0]*(1/CW_{\max}{}^2 + 2(CW_{\max}-1-j)/CW_{\max}{}^2), \quad j \in [CW_{\min}, CW_{\max}-1] \tag{11}$$

C. Calculation of System Throughput

In order to calculate the throughput, we first list our notations for the important parameters in Table 1:

Table 1: Notations of parameters

T_{SP}	time cost by successfully transmitted payloads, excluding backoff time
T_S	time cost by successfully transmitted packets, including backoff time
T_C	time cost by collisions, including backoff time
N_{SP}	number of successfully transmitted packets
Payload	Payload in bits, including UDP IP LLC headers, excluding MAC header.
LinkRate	The link rate in bps
t_C^*	Basic time cost of a collision ,excluding backoff time

t_S^*	Basic time cost of a successful transmitted packet, excluding backoff time
UPay	UDP payload, the real 'data', excluding any headers, maximum is 1472*8 in this research.
MacP	Mac frame length in a PSDU, including Payload plus FCS and/or all other tails on the MAC layer.
ACK	Ack frame length on the MAC layer
N_{Sbl}	number of symbols needed to encode a MAC layer data, only for 802.11g
$SRate$	Symbol encoding rate, only for 802.11g.

In this paper, we define the throughput as in equation (12),

$$Throughput = \frac{T_{SP}}{T_S + T_C} = \frac{N_{SP} \times Payload / LinkRate}{T_S + T_C}, \quad (12)$$

where N_{SP} $Payload$, T_S and T_C can be calculated by:

$$N_{SP} = TotalRound \times (1 - q_0), \quad (13)$$

$$Payload = (LLC + IP + UDP) Header + UPay, \quad (14)$$

$$T_C = TotalRound \times q_0 \times \sum_{i=0}^{CW_{max}-1} p_i (i \times SlotTime + t_C^*), \quad (15)$$

$$T_S = TotalRound \times (1 - q_0) \times \sum_{i=0}^{CW_{max}-1} p_i (i \times SlotTime + t_S^*), \quad (16)$$

For the calculation of t_C^* and t_S^*, the 802.11b and 802.11g protocol should be treated respectively:

For 802.11b, t_C^* and t_S^* can be expressed as:

$$t_C^* = T_{PLCP} + MacP / LinkRate + DIFS + PROP, \quad (17)$$

$$t_S^* = t_C^* + SIFS + T_{PLCP} + ACK / AckRate + PROP, \quad (18)$$

$$MacP = Header(MAC + LLC + IP + UDP) + UPay + FCS, \quad (19)$$

$$T_{PLCP} = PLCPpreamble / PreambleRate + PLCPheader / HeaderRate, \quad (20)$$

For 802.11g, every 216 bits are encoded into one symbol when the Link rate is 54Mbps, t_C^* and t_S^* can be expressed as:

$$t_C^* = PLCP / PlcpRate + N_{sbl} \times SRate + DIFS + PROP \quad (21)$$

$$t_S^* = t_C^* + SIFS + PLCP / PlcpRate + ACK / AckRate + PROP \quad (22)$$

$$MAC = Header(MAC + LLC + IP + UDP) + UPay + FCS + Service + Tail, \quad (23)$$

$$N_{Sbl} = \lceil MAC / SymbolSize \rceil, \quad (24)$$

where $SRate$ is 4μs/symbol and $SymbolSize$ is 216 bits in the 802.11g standard, and N_{Sbl} accounts for the number of symbols needed to encode a MAC layer data unit.

The system throughput can then be calculated by equations (12)-(24).

IV. Model Validation

To validate our analytical model, we conduct simulation studies on 802.11 point-to-point link. Two wireless stations are configured in ad hoc mode and both of them generate saturated UDP traffic. We report the results of 802.11b and 802.11g WLANs in which the RTC/CTS scheme is disabled. Table 2 lists the of the PHY and MAC parameters used in 802.11b and 802.11g standard.

A. *Throughput Analysis of 802.11b*

In this paper, our parameters in simulation and analytical model are all set according to the 802.11 standard. Fig. 4 plots the throughput of 802.11b point-to-point link with different payload sizes. We can observe that our analytical model results are exactly the same as simulation results. We also compare our model to Bianchi's model [5] in terms of throughput, under the set of PHY and MAC parameters in Table 2. It is obvious that Bianchi's model deviate from the simulation results a little bit. This is because Bianchi's model assumes a constant and independent collision probability, which is only accurate when there are a large number of stations in the network.

Meanwhile, in Fig. 4 we also present the throughput when CW_{max} is set to 1024. The throughput of CW_{max} = 1024 is slightly lower than the throughput of CW_{max} = 64, though the difference is negligible. In another word, our model can approximate the system of CW_{max} = 1024 much better than Bianchi's model, though we assume $CW_{max} = 2CW_{\min}$.

B. *Throughput Analysis of 802.11g*

Fig. 5 shows the throughput results of 802.11g. Similar to 802.11b, our model is precise, while Bianchi's model deviates from the simulation results a lot. A special phenomenon in this figure is that the curve has a sawtooth shape, mainly due to the feature of symbol encoding in 802.11g. When sending a packet, 802.11g encodes every 216 bits into one symbol; if the payload is not a multiple of 216 bits, 802.11g adds padding bits. The padding bits are considered as overhead and not counted in our calculation of throughput.

Another observation is that, the throughput of CW_{max} = 1024 is slightly lower than the throughput of CW_{max} = 32. This is because there are only two stations competing for the wireless channel.

Table 2 IEEE 802.11b and 802.11g parameters [1] [2]

	802.11b	802.11g
SlotTime	20 μs	20μs (in ad hoc mode)

SIFSTime	10 µs	10 µs
DIFS	28 µs	28 µs
aCWmin	32	16
aCWmax	1024	1024
PLCP Preamble	72 bits	N.A.
PreambleRate	1 Mbps	N.A.
PLCP Header	48 bits	20 bits
HeaderRate	2 Mbps	N.A.
Service + Tail	N.A.	16 bits + 6 bits
MAC_Header	192 bits	192 bits
LinkRate	11 Mbps	54 Mbps
AckRate	2 Mbps	24 Mbps
Symbol Rate	N.A.	4 µs/symbol
SymbolSize	N.A.	216 bits

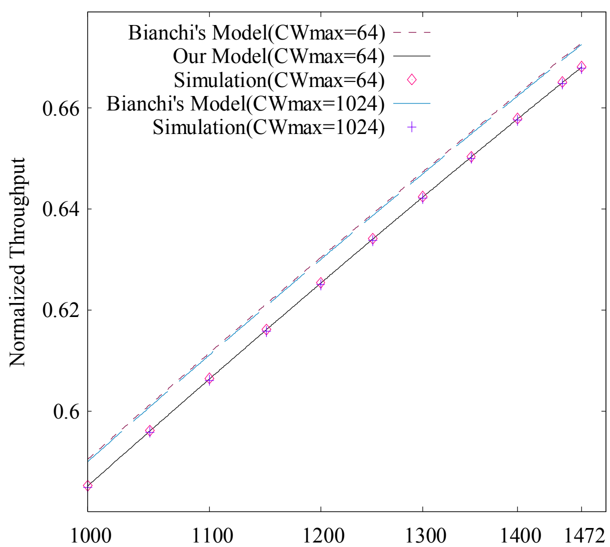

Figure 4: Normalized Throughput of 802.11b

V. Conclusions

In this paper, we proposed a precise Markov model to analyze link performance in IEEE 802.11 Point-to-Point networks. This model focuses on the analysis of system idle time caused by the random backoff period. We demonstrate that our model is precise for the case of $CW_{max} = 2\,CW_{min}$, and it also approximates $CW_{max} = 2^m CW_{min}$ for other values of m much better than Bianchi's model.

Acknowledgement

This work is supported by Hong Kong RGC under grants HKBU 210406, Hong Kong RGC Central Allocation grant HKBU 1/05C, and Hong Kong Baptist University under grant FRG/06-07/II-69.

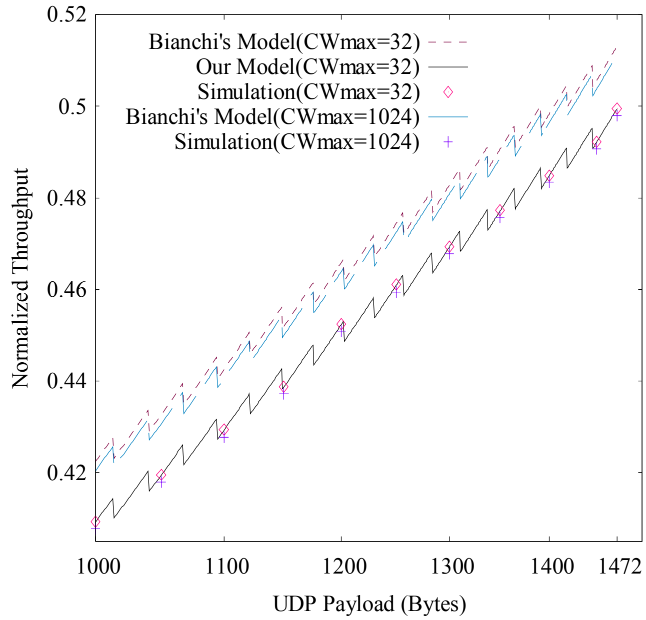

Figure 5: Normalized Throughput of 802.11g

References

[1] ANSI/IEEE Standard 802.11, 1999 Edition, Part 11: Wireless LAN Medium Access Control (MAC) and Physical Layer (PHY) Specifications.

[2] IEEE 802.11 part 11: Wireless LAN medium access control (MAC) and physical layer (PHY) specifications, Amendment 4: Further higher data rate extension in the 2.4GHz Band, June 2003.

[3] Yang Xiao, "IEEE 802.11n: enhancements for higher throughput in wireless LANs," IEEE Wireless Communications, December 2005.

[4] F.Calì, M. Conti, E. Gregori, "IEEE 802.11 wireless LAN: capacity analysis and protocol enhancement", in Proc. of IEEE Infocom'98, pages 142-149, March 29 - April 2, 1998.

[5] Giuseppe Bianchi, "Performance analysis of the IEEE 802.11 distributed coordination function", *IEEE Journal on Selected Areas in Communications*, Vol. 18, NO. 3, pages 535–547, March 2000.

[6] R. Karrer, A. Sabharwal, and E. Knightly, "Enabling large-scale wireless broadband: the case for TAPs," in Proc. of HotNets, Cambridge, MA, 2003.

[7] I. F. Akyildiz, X. Wang, and W. Wang, "Wireless mesh networks: a survey," Computer Networks Journal (Elsevier), vol. 47, no. 4, pp. 445-487, March 2005.

[8] A. Raniwala and T. cker Chiueh, "Architecture and algorithms for an IEEE 802.11-based multi-channel wireless mesh network," in Proc. of IEEE Infocom'05, 2005.

[9] P. Kyasanur and N. Vaidya, "Capacity of multi-channel wireless networks: Impact of number of channels and interfaces," in Proc. of Eleventh ACM MobiCom'05, 2005.

[10] P. Kyasanur, J. So, C. Chereddi, and N. Vaidya, "Multi-Channel mesh networks: challenges and protocols", in IEEE Wireless Communications, April 2006.

[11] J. Shi, T. Salonidis, and E. Knightly, "Starvation mitigation through MultiChannel coordination in CSMA multihop wireless networks," in Proc. of ACM MobiHoc'06, 2006.